Polish Society of Composite Materials
Polskie Towarzystwo Materiałów Kompozytowych

23: 3 (2023) 136-144

COMPOSITES THEORY AND PRACTICE
ISSN: 2084-6096
ISSN (online): 2299-128X

**Dinesh Kumar*, Satnam Singh, Surjit Angra**

*Mechanical Engineering Department, NIT Kurukshetra, Haryana-136119, India*
**Corresponding author. E-mail: dinesh_61900120@nitkkr.ac.in*

*Received (Otrzymano) 8.04.2023*

# ANALYTICAL VERSUS EXPERIMENTAL INVESTIGATION OF PHYSICAL AND MECHANICAL CHARACTERISTICS OF STIR CAST HYBRID ALUMINIUM NANOCOMPOSITE

**Aluminium alloys have good mechanical and physical properties and are lightweight, easy to cast, and simple to machine. Aluminium alloys are widely used in the aviation industry, auto sector, defence sector, and structural industries because of their promising abilities. The fundamental aim of this study was to investigate the mechanical properties and physical characteristics of a stir cast hybrid aluminium nanocomposite reinforced with 1-3 wt.% cerium oxide ($CeO_2$) and graphene nanoplatelets (GNPs). Utilizing SEM, microstructural analysis was carried out. The existence of the elements of the reinforcement in the manufactured nanocomposite specimens was verified using EDAX. With an increase in the reinforcement wt.%, improvements in the mechanical and physical properties were seen. In the hybrid nanocomposites reinforced with 3 wt.% GNPs and 3 wt.% $CeO_2$, a low porosity of 1.06% was observed. The best results for tensile strength, yield strength, and microhardness were 398 MPa, 247 MPa, and 119.6 HV, respectively. The SEM micrographs of the studied materials showed that the reinforcement particles were uniformly dispersed and refined into ultrafine grains.**

**Keywords:** **aluminium nanocomposite, density, porosity, microhardness, tensile strength, TEM analysis, SEM analysis, grain size analysis**

## INTRODUCTION

Modern, innovative materials are needed now more than ever as the aerospace and automotive sectors are experiencing a surge in demand. This circumstance calls for a specially created combination of materials with distinctive and unique properties [1]. Modern composite materials can support the achievement of these goals. Currently, traditional composites are being supplanted by hybrid composites. Due to their improved performance and dependability, hybrid composites have a high potential for engineering applications [2].

A hybrid composite material is one that is created from two or more different components and has unique microscopic properties, in addition to physical and chemical characteristics in comparison to the base material. A variety of distinctive qualities, including a high strength-to-weight ratio (SWR), high stiffness, high wear resistance, among others [3], are present in the newly fabricated hybrid composite. Aluminium is the second-most widely available metal in the Earth's core [4]. Since 1990, the majority of engineering fields, such as aerospace, marine, automotive, and structural, have historically used aluminium and its alloys. Metal matrix composites (MMC) are the result of the addition of small quantities of reinforcement to a metal matrix material [5]. Hybrid aluminium metal matrix composites (HAMMC) combine two or more ceramic or non-ceramic elements in weight or volume proportions with aluminium or aluminium alloys. Nanocomposite materials refer to a solid structure reinforced with nanoscale-sized particles [6]. The popularity of hybrid aluminium nanocomposites (HANC) in a variety of sectors is due to their improved customised tribo-mechanical characteristics. Additionally, HANC offer a technologically advanced, adaptable platform for value-added applications like photovoltaic cells, solid-state batteries, biosensors, light-emitting devices, lightweight structures, and lithium-ion batteries [7]. The maximum solubility of an element in metal is described by the metallurgist William Hume-Rothery. In order to improve the characteristics of hybrid nanocomposite materials, the selection of the matrix material and the dispersion of the reinforcement are crucial [8]. For usage as reinforcement, a variety of ceramic and non-ceramic nanoparticles are available. Reinforcement materials include alumina, silicon carbide, boron nitride, titanium boride, and carbon nanotubes [9]. The choice of appropriate manufacturing processes comes in second on the list of important factors.

Traditional casting techniques have intrinsic process capabilities and process-oriented flaws as their drawbacks. These conventional casting procedures also have an impact on the general quality of the material that is

manufactured. Casting imperfections that impact the mechanical and microstructural characteristics of cast components include shrinkage, slag inclusion, blowholes, pores, and dendritic formations [10]. Advanced casting processes, including squeeze casting, powder metallurgy, spray decomposition, and friction-stir processing, can be employed to prevent such flaws and issues during casting. When it comes to obtaining a uniform dispersion and solid bonding of the reinforcing particles, the stir casting process is quite successful [11-13].

Jaber Abu Qudeiri et al. investigated the impact of the reinforcement on an Al-6061 metal matrix composite made using the stir casting technique. Their research found that the porosity also had an effect on the mechanical properties because of fractures, micropores, and other faults in the produced composite [14]. Satnam Singh et al. utilized stir casting to create a Al6061-5% Gr-5% SiC hybrid composite. It was discovered that (5%) was the acceptable degree of porosity, above which the mechanical strength of the resultant composites decreased [15].

An Al6061-GO/CNT composite was created by Virat Khanna et al. utilizing the stir casting process, and they came to the conclusion that the consistent dispersion and excellent cohesive features of the GO/CNT were what caused the increase in strength [16]. M. Penchal Reddy et al. stated that with 1.5 vol.% TiC in the AMMC, the highest values of microhardness of 89.6 HV and 151.2 MPa yield strength were observed. With a reinforcement of 1.5 vol.% TiC in the AMMC, the percent elongation, tensile, and compressive strengths were also discovered to be at their highest [17].

In the current study, due to their low density and high melting temperature, respectively, cerium oxide and graphene nanoplatelets were chosen as the reinforcement materials in the research [18]. Owing to its lightweight, low density, and low melting point characteristics, Al-6061 was utilised as the matrix material. It may also be used to create ternary and quaternary engineering alloys. This study assessed the mechanical and physical properties. The highlights of the current study are listed below:

- The liquid metallurgy route was used to prepare the hybrid aluminium metal matrix nano-composites reinforced with cerium oxide and graphene nanoplatelets.
- Using the rule of mixtures, the densities were examined and the experimental values were compared to the theoretical values.
- The mechanical characteristics were analysed using Cahoon's equation.
- The mechanical properties were enhanced by the homogenous dispersion of the reinforcing particles, as shown by SEM analysis.
- EDAX analysis identified the elements present in the produced composites, along with their varying concentrations.

## MATERIALS AND METHODS

The matrix material was an alloy called Al-6061. The chemical constituents of the Al-6061 alloy were examined using a Spectro-analyser, as presented in Table 1.

TABLE 1. **Chemical composition of Al-6061 alloy**

| Element | Si | Fe | Cu | Mn | Mg |
|---|---|---|---|---|---|
| % | 0.51 | 0.257 | 0.219 | 0.043 | 0.797 |
| **Element** | **Cr** | **Ni** | **Zn** | **Ti** | **Al** |
| % | 0.157 | 0.001 | 0.094 | 0.027 | Bal |

Cerium oxide ($CeO_2$) and graphene nanoplatelets (GNPs) were employed as the nano-reinforcements; Table 2 lists their characteristics.

TABLE 2. **Characteristics of matrix and nano-reinforcements**

| Reinforcement/ Matrix | Purity of powder [%] | Mean particle size [nm] | Melt temperature [°C] | Density [g/cm$^3$] |
|---|---|---|---|---|
| $CeO_2$ | 99.5 | 3-6 | 3670 | 7.2 |
| GNPs | 99.9 | 24-28 | 2400 | 2.3 |
| Al-6061 alloy | 98.0 | - | 750 | 2.71 |

To produce the test specimens, nano-reinforcement particles in the range of 1-3 wt.% were used. The mechanical and physical characteristics of the produced specimens were evaluated. The morphology of the raw material was also analysed using transmission electron microscopy (TEM), as shown in Figure 1.

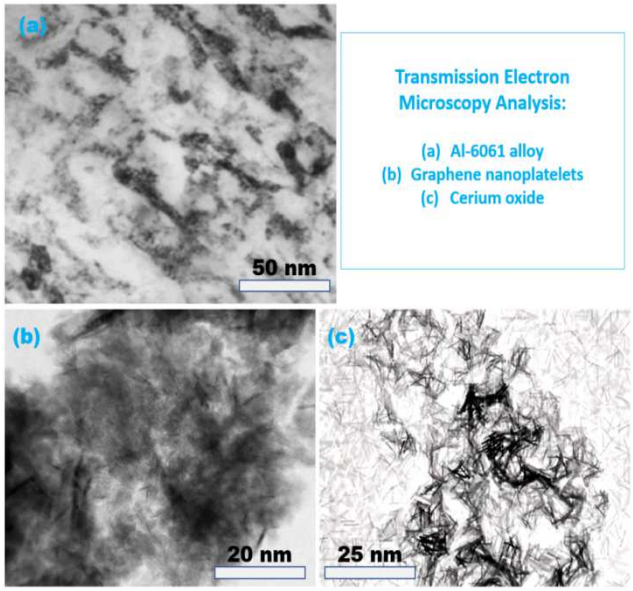


Fig. 1. TEM analysis of raw materials: a) Al-6061, b) GNPs, and c) $CeO_2$

The HANC specimens were made using the stir casting method, and Figure 2 shows the stir casting

 

process flow diagram. In an electric furnace, the Al-6061 alloy was melted to 810°C. The nano-reinforcements were placed in an aluminium foil envelope and warmed in a muffle furnace for 40 minutes at 300°C. The preheating procedure minimised the temperature difference after adding the particles to the molten metal, as well as reduced the moisture content and absorbed gases in the reinforcements [19].

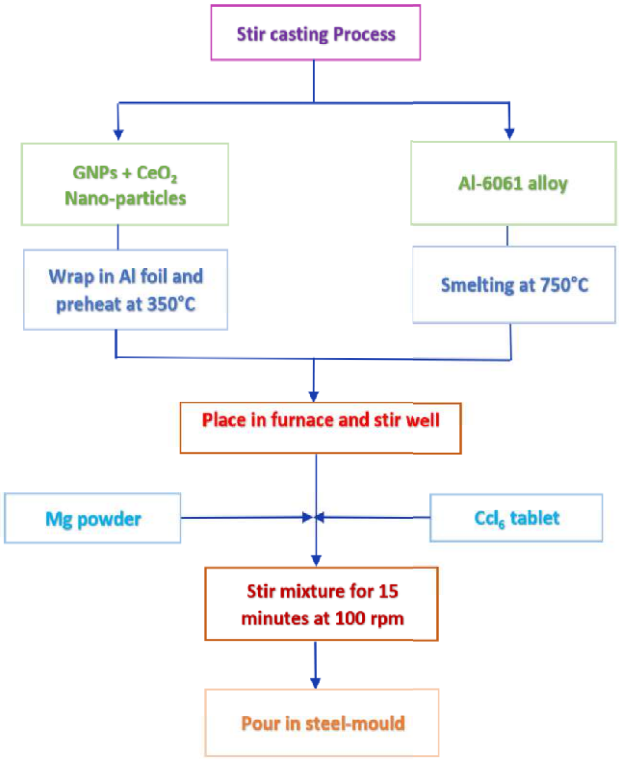


Fig. 2. Stir casting method for fabrication of HANC

Degassing the molten metal required the application of a hexachloroethane ($ccl_6$) tablet. In the degassing process, inert gases are injected into aluminium melts to eliminate hydrogen and avoid eventual porosity in cast pieces. The addition of ccl6 tablets reduces the pores and holes in the cast composites. The molten metal was kept at a temperature of 750°C with a suitable viscosity. It was stirred at 350 rpm for 15 min using a diamond-coated impeller to produce a suitable vortex [20]. To create a strong enough vortex for uniform mixing of the nano-reinforcement particles with the molten metal, a high stirring speed was employed. In addition, the stirring speed needs to be low enough to prevent gas and air from being trapped in the liquid pool.

Magnesium was added at a content of 2 wt.% to improve the wettability of the reinforcing particles [21]. To ensure that the particles were mixed evenly, the stirring speed was kept at 300 rpm for the next 10 minutes, then decreased to 200 rpm for the next 5 minutes. Figure 3a displays the pouring of the molten material into the mould, followed by its cooling and solidification (b), removal from the mould (c), and the finally cast specimens (d). The specimens were then heat treated to the optimal T6 level to improve their mechanical properties [22]. The specimens were quenched in water by solutionizing at 560°C for 3 hours, then artificially aged for 5 hours at 150°C. The stir casting method was used to create four specimens with various compositions, as indicated in Table 3.


Fig. 3. a) Pouring in mould, b) solidification of molten metal, c) unmoulded cast specimens, and d) finished cast specimens

TABLE 3. **Nomenclature of fabricated specimens**

| Specimen | Nomenclature | Composition |
|---|---|---|
| 1 | NC01 | Al-6061/0GNPs/0$CeO_2$ |
| 2 | NC02 | Al-6061/1GNPs/1$CeO_2$ |
| 3 | NC03 | Al-6061/2GNPs/2$CeO_2$ |
| 4 | NC04 | Al-6061/3GNPs/3$CeO_2$ |

## TESTING AND CHARACTERIZATION

Field emission scanning electron microscopy (FESEM) was used to perform the microstructure examination of the micro sub-surface of the produced HANCs for information about their microstructure. By analysing the HANCs, we were able to learn about the phase distribution and its type in the produced composites, as well as the nature of dispersion of the reinforcement in the matrix material. By applying Archimedes' principle, the ASTM D792 standard was applied to measure the experimental density of the composites [23]. On the other hand, the rule of mixtures was used to determine the theoretical density. The porosity of the produced composites was determined once the two densities (theoretical and experimental) were obtained. Equation (1) can be used to obtain the theoretical density of the hybrid composite [24]:

$$\rho_{HANCs} = \rho_{Al} W_{Al} + \rho_{GNPs} W_{GNPs} + \\ + \rho_{CeO_2} W_{CeO_2} \quad (1)$$

where $\rho_{Al}$, $W_{Al}$, $\rho_{GNPs}$, $W_{GNPs}$, $\rho_{CeO_2}$, and $W_{CeO_2}$ are the densities and weight percentages of Al-6061, GNPs, and $CeO_2$, respectively.

Equation (2) can be used to calculate the relative density (%) [25]:

 

$$\text{Relative density (\%)} = \frac{\rho_{Exp.}}{\rho_{Theo.}} x\ 100 \quad (2)$$

$\rho_{Exp.}$ – experimental density, and $\rho_{Theo.}$ – theoretical density.

Equation (3) can be used to determine the porosity of the specimens (%), as shown below [26]:

$$\text{Porosity} = 100\% - \text{Relative density (\%)} \quad (3)$$

Before conducting the Vickers hardness test, the test specimens were cleaned and polished. A load of 200 g was applied on ten locations for a dwell time of 20 seconds; the average was then calculated and recorded. Cahoon's Equations (4) and (5) were used to calculate the tensile strength and yield strength, which were acknowledged by Adebiyi et al. [27], Annaz et al. [28], Irhayyim et al. [29-31], and Popoola et al. [32-34] as well as recommended and suggested by Cahoon et al. [35, 36].

$$TS = \frac{VH}{2.9}\ x\ \left(\frac{m}{0.217}\right)^m \quad (4)$$

$$YS = \frac{VH}{3}\ x\ 0.1^m \quad (5)$$

*VH*, *m*, *YS*, and *TS* are the respectively the Vickers hardness [MPa], strain hardening exponent, yield strength [MPa], and tensile strength [MPa]. According to Callister and Rethwisch [37], m should be smaller than unity, and in the current investigation, it was set at 0.02.

## RESULTS AND DISCUSSION

### Physical properties

The predicted and actual densities of the HANC specimens made using the stir casting method are represented graphically in Figure 2. Because the stir cast HANCs have higher theoretical densities than experimental densities, the analysis demonstrates their denser nature. The calculation for the theoretical densities of the HANC specimens may be generated using the following equations:

$$\rho_{NC01} = 2.71 \text{ x } 1.00 + 7.2 \text{ x } 0 + 2.3 \text{ x } 0 = \\ = 2.71 \text{ g/cm}^3 \quad (6)$$

$$\rho_{NC02} = 2.71 \text{ x } 0.98 + 7.2 \text{ x } 0.01 + 2.3 \text{ x } 0.01 = \\ = 2.751 \text{ g/cm}^3 \quad (7)$$

$$\rho_{NC03} = 2.71 \text{ x } 0.96 + 7.2 \text{ x } 0.02 + 2.3 \text{ x } 0.02 = \\ = 2.792 \text{ g/cm}^3 \quad (8)$$

$$\rho_{NC04} = 2.71 \text{ x } 0.94 + 7.2 \text{ x } 0.03 + 2.3 \text{ x } 0.03 = \\ = 2.821 \text{ g/cm}^3 \quad (9)$$

where $\rho_{Al}$, $\rho_{GNPs}$, $\rho_{CeO_2}$ are the densities of the Al-6061, graphene nanoplatelets, and cerium oxide, $W_{Al}$ $W_{GNPs}$ and $W_{CeO_2}$ the weight percentages of the Al-6061, graphene nanoplatelets, and cerium oxide, respectively. Table 2 presents the matrix and nano-reinforcement densities. The findings of the density values obtained from Equations $6^t$ to $9^t$ presented above and the physical properties are listed in Table 4 for the composite densities for 0, 1, 2, and 3 weight percent GNPs and $CeO_2$. Figure 4 displays a graphical representation the physical properties, including porosity in addition to theoretical and experimental densities. As the amount of nano-reinforcements increased, the physical properties also increased linearly.

TABLE 4. **Physical properties of HANC specimens**

| Specimen | $\rho_{Theo.}$ [g/cm$^3$] | $\rho_{Exp.}$ [g/cm$^3$] | Relative density [%] | Porosity [%] |
|---|---|---|---|---|
| NC01 | 2.680 | 2.710 | 98.893 | 1.107 |
| NC02 | 2.725 | 2.751 | 99.062 | 0.938 |
| NC03 | 2.776 | 2.792 | 99.427 | 0.573 |
| NC04 | 2.821 | 2.833 | 99.576 | 0.424 |

Figure 4 illustrates the relationship between the relative density and porosity of the manufactured HANC specimens. The theoretical data (Table 3) demonstrate that a decrease in the nano-reinforcement wt.% lowers the porosity and raises the density of the material. The plotting of both physical properties results in an x-shaped graph, indicating that they are inversely proportional to one another. As the weight percentage of $CeO_2$ and GNPs increased, it was possible to observe a rise in the relative density of the manufactured hybrid composite. The reduction in porosity might be caused by the homogeneous dispersion of both nano-reinforcements. When compared to NC01, the porosity of the NC04 specimen declined by 61.7%.

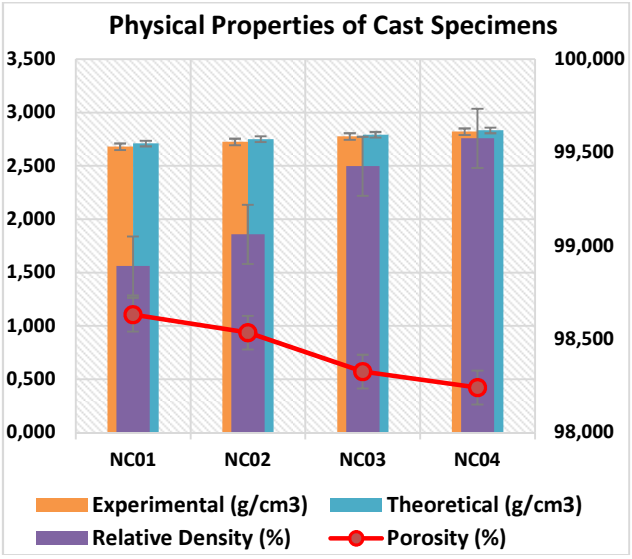


Fig. 4. Physical properties of HANCs

Vipin Kumar Sharma et al. fabricated a hybrid aluminium composite with 2.5 wt.% silicon carbide (SiC), 2.5 wt.% alumina ($Al_2O_3$), and 0.5, 1.5, 2.5 wt.% cerium oxide ($CeO_2$) in the Al-6063 alloy using the stir casting method. The investigation revealed that the least amount of porosity, highest homogeneity and the most refined grains were observed after adding the amount of 2.5 wt.% cerium oxide. With an increase in the weight percentage of various reinforcements, it was discovered that the microhardness of the hybrid aluminium composites grew [38]. M. Rajabi et al. utilized a Y-shaped mixer to disperse nano zirconium dioxide ($nZrO_2$) particles in aluminium powder. The quantity of $nZrO_2$ reinforcement varied from 3 to 15 wt.% with an average particle size of 40 nm. According to the conclusions, an increase in the reinforcement wt.% was associated with a corresponding rise in porosity and a fall in the density of the composite, respectively. A higher bulk density (2.53 g/cm$^3$) was achieved in the produced aluminium nanocomposite at the $nZrO_2$ content of 6 wt.% [39].

According to Bhubnaeswar et al., the hardness of the manufactured stir cast composite rose when 5, 10, 15, and 20 wt.% SiCp reinforcement was added to the Al6061 matrix. When the produced composite is compared to the pure aluminium alloy, there was an 18% improvement in hardness with the addition of 15 wt.% SiC reinforcement in the Al-6061 alloy [40]. An Al6063-xTiC MMC was produced by Venkateshwar et al. utilizing the stir casting method. The MMC was created using Al6063 and 5, 10, and 15 wt.% TiC. In comparison to the unreinforced Al6063 alloy, which has a hardness of 59.6 HV, the manufactured composite attained 99.6 HV [41]. Hardness tests were conducted on MMCs made from the combination of Al alloy and SiC reinforcement by Yashpal et al. The homogenous dispersion of SiC particles in the matrix material was reported to significantly increase the mechanical parameters such as the yield strength, Young's modulus, and hardness [42]. Using the stir casting process, Chaubey et al. reported that owing to the presence of SiC particles in the Al-5083 composite, the hardness value improved to 85 BHN from 52 BHN when reinforced with SiC particles by means of the stir casting process. The 85% growth in hardness in the fabricated material extends the service life and improves the wear resistance [43].

The porosity values in the current study are strictly within the permitted range and strictly follow the trend of other investigations. As the weight percentage of the reinforcements (GNPs and $CeO_2$) added to the Al-6061 alloy increased, so did the relative density (the ratio of theoretical to experimental density). A smooth surface and uniform dispersion of the reinforcement particles in the fabricated HANCs was observed with an increase in the weight percentages of GNPs and $CeO_2$ [44-47].

## Mechanical properties

Figure 5 shows the yield strength, tensile strength, and microhardness of the test specimens. When Al-6061 was supplemented with 1 wt.% GNPs and 1 wt.% $CeO_2$, an increase from 52 HV (Al-6061 alloy) to 96.9 HV was observed. With the addition of 2 wt.% $CeO_2$ + 2 wt.% GNPs and 3 wt.% GNPs + 3 wt.% $CeO_2$ reinforcement to the matrix material, further increments to 105.5 HV and 119.6 HV, respectively, were seen in comparison to the base alloy.

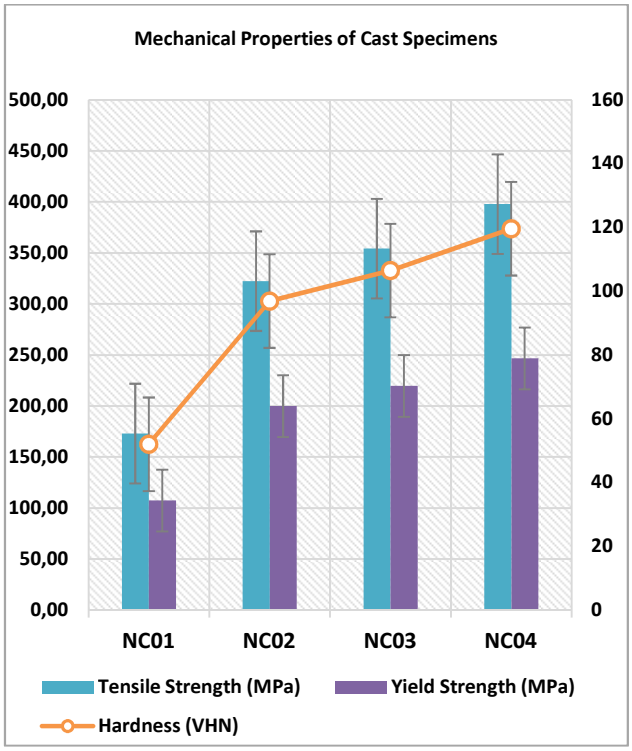


Fig. 5. Mechanical properties of HANC specimens

In comparison to earlier studies, a rise in microhardness values was seen. Multi-wall carbon nanotubes (MWCNTs) were added to the Al-6061 alloy, which resulted in an improvement in the mechanical properties. Prakash et al. concluded that the addition of 1.5 weight percent MWCNTs raised the microhardness, tensile strength, and impact strength of MMCs by 18.6%, 11.93%, and 66.6%, respectively. Proper MWCNT distribution in the Al-6061 alloy matrix can be seen in scanning electron microscopy analysis [48]. Cerium oxide ($CeO_2$) is a rare-earth particle that Vipin Kumar Sharma and colleagues noticed to have an impact on hybrid composites. 2.5 weight percent $CeO_2$ results in the best mechanical qualities, such as an increase in microhardness of 17.02%, growth in tensile strength from 30 to 123 MPa, and a rise in flexural strength from 340 MPa to 615.6 MPa. With 2.5 wt.% $CeO_2$ added to the hybrid composite, an increase in the wear rate of 87.28% was also noted [49]. The mechanical properties of the manufactured HANC specimens are shown in Table 5.

 

TABLE 5. **Mechanical properties of HANC specimens [35, 36]**

| Specimen | Micro-hardness [HV] | Tensile strength [MPa] | Yield strength [MPa] | Grain size [nm] |
|---|---|---|---|---|
| NC01 | 52 | 173.004 ± 0.6 | 107.255 ± 0.8 | 29.70 |
| NC02 | 96.9 | 322.386 ± 0.4 | 199.866 ± 0.6 | 22.84 |
| NC03 | 106.5 | 354.325 ± 0.7 | 219.667 ± 0.5 | 14.27 |
| NC04 | 119.6 | 397.909 ± 0.2 | 246.687 ± 0.1 | 6.36 |

Additionally, the NC04 specimen had the highest tensile strength at 397.909 ± 0.2 MPa. The tensile strength of the NC01 specimen, amounting to 173.004 ± 0.6 MPa, was the lowest. The tensile strength was improved thanks to the effects of different stir casting conditions. Baradeswaran et al. created an MMC from Al7075, 5 wt.% graphite (Gr), and 2, 4, 6, and 8 wt.% $Al_2O_3$. Compared to the pure Al alloy, the 238 MPa tensile strength that was achieved is an increase of 11% [50]. At various temperatures, Kumar et al. cast a composite made of an A356 aluminium alloy with 6% $TiB_2$. Pouring temperatures of 750, 780, and 810°C were selected. When the molten metal was poured, the effect of the pouring temperature on microhardness was seen. The microhardness was seen to rise linearly with a rising pouring temperature [31]. An Al6061-5 wt.% Gr MMC was made by Saravanan et al. employing the stir casting method. The tensile strength grew from 97 MPa to 249 MPa, a 157% increase over the base Al6061 alloy [51]. Using the stir casting technique, Surabhi et al. found increased tensile strength of an Al7075-TiC (5, 10, and 15 wt.%) MMC due to the homogeneous dispersion of the TiC particles. There was a steady pattern up to 10 wt.% TiC, but after that, the tensile strength started to decrease [52].

Furthermore, A. Momeni et al. reported that stir cast composite material with 1.5 wt.% $nSiC_p$ in the A356 aluminium alloy had improved tensile and compressive strengths [53]. Abdizadeh and Baghchesara fabricated stir cast A356-15% $ZrO_2$ MMCs produced at 750°C, which resulted in a UTS of 232 MPa. For the same MMC composition, increments in the density and microhardness of 10% and 52%, respectively, were also noted [54]. Following the same trend as stated in the previous studies, the highest yield strength of the NC04 specimen was 246.687 ± 0.1MPa, which was 130% more than the base material (107.255 ± 0.8 MPa). According to the observations in the current work, the uniform dispersion results in an improvement in the mechanical properties.

## Microstructural studies

The SEM and EDAX analyses of the manufactured HANC specimens with GNPs and $CeO_2$ nanoparticles in the matrix material are shown in Figure 6. In the SEM micrographs, four distinct regions could be distinguished: a grey zone representing the matrix (Al-6061 alloy), a white region representing cerium oxide, and a black region representing GNPs. Last but not least, the porosity content of the HANC specimens is shown by the dark grey colour. The microstructure was observed to have changed as a direct result of the incorporation of the nano-reinforcements. When compared to the base material, the HANC specimens can be seen to have a more uniform dispersion and a morphology that is devoid of defects.

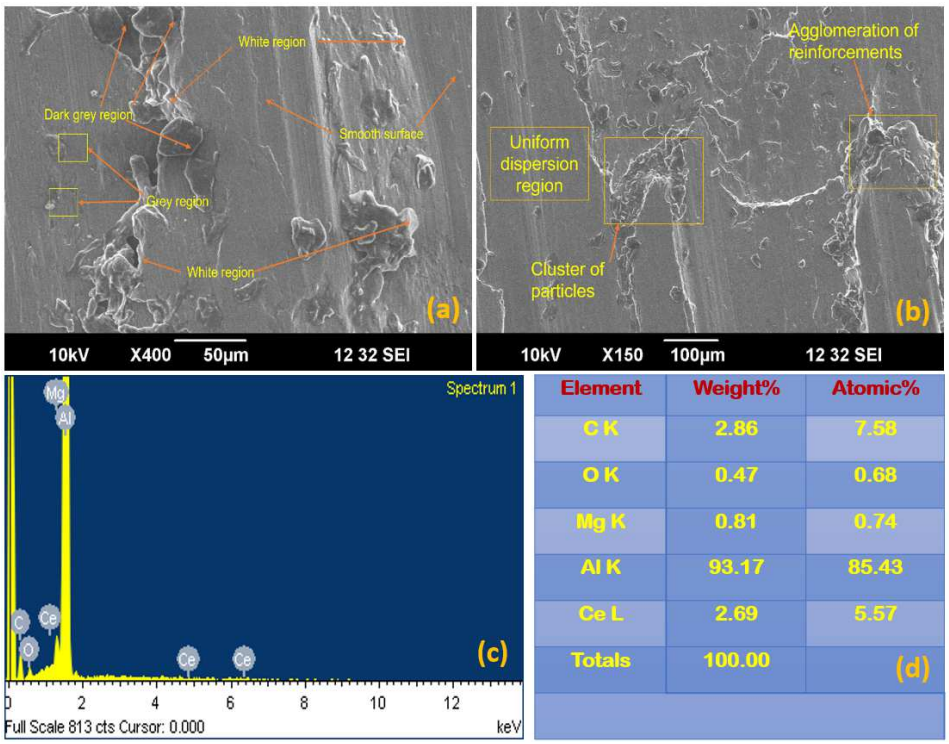


Fig. 6. SEM micrographs of specimens: a) NC02, b) NC04, c) EDAX spectrum of NC04, d) EDAX with element wt.% of NC04 specimen

 

The EDAX analysis verifies the presence of the GNPs and $CeO_2$ nano-particles. The addition of the magnesium powder was done in order to improve the wettability of the reinforcement by the matrix, which in turn enhances the wettability of the hybrid nanocomposites that were formed [55, 56]. Tablets of hexachloroethane were also employed for degassing during stir casting of the HANC specimens [57]. Earlier research concurred with the findings of the most recent work, according to which the enhancement of the interfacial bonding of the matrix and reinforcement can be interpreted as an improved microstructural feature of the HANCs.

Bhoi et al. noticed strong bonding and homogeneous reinforcement distribution in an Al-$Y_2O_3$ composite. Due to the high density and load transmission capabilities of the produced composites, the Orowan strengthening effect was also noted [58]. SEM was used to confirm the uniform distribution and good bonding of the $Y_2O_3$ particles with the Al matrix. The behaviour of Al2024 reinforced with various weight percentages of $Y_2O_3$ from 0% to 20% in intervals of five was explained by Hamada et al. Up to 10 wt.%, there was an even distribution of reinforcement, but after that point, certain yttria particles began to aggregate and cluster, which increased the porosity of the 15 and 20 wt.% composites [24]. The Al6061/SiC/($CeO_2$+$La_2O_3$) hybrid composite was said to have a homogeneous distribution of reinforcements with strong interfacial bonding, acceptable grain refinement, and low porosity [59]. The present study continues these trends by enhancing the fluidity of the molten metal and the mechanical properties of the HANCs by adding GNPs and $CeO_2$. Additionally, SEM demonstrated that in the produced HANC specimens, the increase in porosity was inversely proportional to the reinforcement content [60-62].

## CONCLUSION

The following conclusions were reached after analysing the physical and mechanical properties, as well as the microstructure of the fabricated nanocomposite:

1. Using the stir casting method, an aluminium nanocomposite reinforced with GNPs and $CeO_2$ nanoparticles was successfully produced.
2. Compared to the unreinforced specimen, the hybrid aluminium composite has superior physical and mechanical properties thanks to the inclusion of GNPs and $CeO_2$ nanoparticles (1-3 wt.%).
3. Both the experimental and theoretical densities were found to be higher after the addition of reinforcement, but the porosity was found to be lower after using the same percentages of GNPs and $CeO_2$. In addition to this, it was observed that the densities and porosities have a relationship that is inversely proportionate to one another.
4. The addition of 3 wt.% GNPs and 3 wt.% $CeO_2$ nanoparticles to the Al-6061 alloy enhanced its Vickers microhardness, tensile strength, and yield strength. The material has a tensile strength of 397.909 MPa, yield strength of 246.687 MPa, and Vickers microhardness of 119.6 HV.
5. The microstructural analysis revealed homogeneous dispersion of the reinforcement in the hybrid aluminium nanocomposite specimens and the fact that they are defect-free. In the fabricated nanocomposites no visible cracks or pores were found. This is because the grain size of the reinforcements in HANCs is more refined, and they also have stronger interfacial bonding.

## REFERENCES

[1] Kumar D., Singh S., Angra S., Effect of reinforcements on mechanical and tribological behavior of magnesium-based composites: a review, Mater. Phys. Mech. 2022, 50, 3, 439--458, DOI: 10.18149/MPM.5032022.

[2] Aravind Senan V.R., Anandakrishnan G., Rahul S.R., Reghunath N., Shankar K.V., An investigation on the impact of SiC/B4C on the mechanical properties of Al-6.6Si-0.4Mg alloy, Mater. Today Proc. 2019, 26, 649-653, DOI: 10.1016/j.matpr.2019.12.359.

[3] Kumar D., Angra S., Singh S., Mechanical properties and wear behaviour of stir cast aluminum metal matrix composite: A review, Int. J. Eng. Trans. A Basics 2022, 35, 4, 794-801, DOI: 10.5829/IJE.2022.35.04A.19.

[4] Kumar S., Kumar A., Vanitha C., Corrosion behaviour of Al 7075/TiC composites processed through friction stir processing, Mater. Today Proc. 2019, 15, 21-29, DOI: 10.1016/j.matpr.2019.05.019.

[5] Gordo E. et al., Corrosion and tribocorrosion behavior of Ti-alumina composites, Key Eng. Mater. 2016, 704, 28-37, DOI: 10.4028/www.scientific.net/KEM.704.28.

[6] Singh S., Angra S., Experimental evaluation of hygrothermal degradation of stainless steel fibre metal laminate, Eng. Sci. Technol. an Int. J. 2018, 21, 1, 170-179, DOI: 10.1016/j.jestch.2018.01.002.

[7] Kumar H., Kumar V., Kumar D., Singh S., Wear behavior of friction stir processed copper-cerium oxide surface, Composites. Theory and Practice 2023, 10, 1, 78-84.

[8] Kumar D., Singh S., Angra S., Morphology and corrosion behavior of stir-cast Al6061-$CeO_2$ nanocomposite immersed in NaCl and $H_2SO_4$ solutions, Evergreen 2023, 10, 1, 94-104.

[9] Ramanathan A., Krishnan P.K., Muraliraja R., A review on the production of metal matrix composites through stir casting – Furnace design, properties, challenges, and research opportunities, J. Manuf. Process. 2019, 42, April, 213-245, DOI: 10.1016/j.jmapro.2019.04.017.

[10] Tamuly R., Behl A., Borkar H., Effect of addition of grain refiner and modifier on microstructural and mechanical properties of squeeze cast A356 alloy, Trans. Indian Inst. Met. 2022, DOI: 10.1007/s12666-022-02607-4.

[11] Gudimetla A., Lingaraju D., Prasad S.S., Investigation of mechanical and tribological behavior of Al 4032-SiHGM MMC, Composites. Theory and Practice 2020, 4, 142-156.

[12] Murugan S.S., Velmurugan V.J.M., Mechanical properties of SiC, $Al_2O_3$ reinforced aluminium 6061-T6 hybrid matrix composite, J. Inst. Eng. Ser. D 2018, 99, 1, 71-77, DOI: 10.1007/s40033-017-0142-3.

 

[13] Weiss D., 50 years of foundry-produced metal matrix composites and future opportunities, Int. J. Met. 2019, 14, 291-317, DOI: 10.1007/s40962-019-00375-4.

[14] Kareem A., Qudeiri J.A., Abdudeen A., Ahammed T., Ziout A., A review on aa 6061 metal matrix composites produced by stir casting, Materials 2021, 14, 1, 1-22, DOI: 10.3390/ma14010175.

[15] Satnam Singh D.K., Angra S., Optimization of hardness and tensile strength of stir cast hybrid aluminum metal matrix composite using grey relational analysis, International Conference on Computational Modelling, Simulation and Optimization (ICCMSO) 2022, 132-136.

[16] Khanna V., Kumar V., Anil S., Mechanical properties of aluminium-graphene/carbon nanotubes (CNTs) metal matrix composites: Advancement, opportunities and perspective, Mater. Res. Bull. 2021, 138, January, 111224, DOI: 10.1016/j.materresbull.2021.111224.

[17] Reddy M.P. et al., Enhancing thermal and mechanical response of aluminum using nanolength scale TiC ceramic reinforcement, Ceram. Int. 2018, January, 0-1, DOI: 10.1016/j.ceramint.2018.02.135.

[18] Bandil K., Vashisth H., Kumar S., Verma L., Jamwal A., Kumar D., Microstructural, mechanical and corrosion behaviour of Al-Si alloy reinforced with SiC metal matrix composite, Journal of Composite Materials 2019, 53, 28-30, DOI: 10.1177/0021998319856679.

[19] Saravanan C., Subramanian K., Krishnan V.A., Narayanan R.S., Effect of particulate reinforced aluminium metal matrix composite – A review, Mechanics and Mechanical Engineering 2015, 19, 1, 23-30.

[20] Ranjan U., Dwivedi S.P., Pandey D., Kumar R., Garg T.K., A critical review on the utilization of SAC and eggshell in the development of aluminium based composite material, Mater. Today Proc. 2021, 47, 3839-3844, DOI: 10.1016/j.matpr.2021.03.179.

[21] Gowrishankar T.P., Manjunatha L.H., Sangmesh B., Mechanical and wear behaviour of Al6061 reinforced with graphite and TiC hybrid MMC's, Mater. Res. Innov. 2020, 24, 3, 1-7, DOI: 10.1080/14328917.2019.1628497.

[22] Alaneme K.K., Bodunrin M.O., Corrosion behavior of alumina reinforced aluminium (6063) metal matrix composites, Journal of Minerals & Materials Characterization & Engineering 2011, 10, 12, 1153-1165.

[23] Bright Singh R.L., Jinu G.R., Manoj M., Perumal A.E., Tribological behaviour of Al8090-SiC metal matrix composites with dissimilar B4C addition, Silicon 2022, 14, 8895-8908, 0123456789, DOI: 10.1007/s12633-021-01608-0.

[24] Hamada M.L., Alwan G.S., Annaz A.A., Irhayyim S.S., Hammood H.S., Experimental investigation of mechanical and tribological characteristics of Al 2024 matrix composite reinforced by yttrium oxide particles, Korean Journal of Materials Research 2021, 31, 6, 339-344.

[25] Abedinzadeh R., Safavi S.M., Karimzadeh F., A study of pressureless microwave sintering, microwave-assisted hot press sintering and conventional hot pressing on properties of aluminium/alumina nanocomposite, J. Mech. Sci. Technol. 2016, 30, 5, 1967-1972, DOI: 10.1007/s12206-016-0402-4.

[26] Awad M., Hassan N.M., Kannan S., Mechanical properties of melt infiltration and powder metallurgy fabricated aluminum metal matrix composite, Proc. Inst. Mech. Eng. Part B J. Eng. Manuf. 2021, 235, 13, 2093-2107, DOI: 10.1177/09544054211015956.

[27] Adebiyi D.I., Popoola A.P.I., Mitigation of abrasive wear damage of Ti-6Al-4V by laser surface alloying, J. Mater. 2015, 74, 67-75, DOI: 10.1016/j.matdes.2015.02.010.

[28] Annaz A.A., Irhayyim S.S., Hamada M.L., Hammood H.S., Comparative study of mechanical performance between Al – graphite and Cu – graphite self-lubricating composites reinforced by nano-Ag particles, AIMS Materials Science 2020, 7, June, 534-551, DOI: 10.3934/matersci.2020.5.534.

[29] Hammood H.S., Mahmood A.S., Irhayyim S.S., Effect of graphite particles on physical and mechanical properties of nickel matrix composite, Periodicals of Engineering and Natural Sciences 2019, 7, 3, 1318-1328.

[30] Irhayyim S.S., Hammood H.S., Mahdi A.D., Mechanical and wear properties of hybrid aluminum matrix composite reinforced with graphite and nano MgO particles prepared by powder metallurgy technique, AIMS Materials Science 2020, 7, December, 103-115, DOI: 10.3934/matersci.2020.1.103.

[31] Irhayyim S.S., Hammood H.S., Abdulhadi H.A., Effect of nano-$TiO_2$ particles on mechanical performance of Al-CNT matrix composite, AIMS Materials Science 2019, 6, September, 1124-1134, DOI: 10.3934/matersci.2019.6.1124.

[32] Ujah C., Popoola P., Popoola O., Aigbodion V., Enhanced mechanical, electrical and corrosion characteristics of Al-CNTs-Nb composite processed via spark plasma sintering for conductor core, Journal of Composite Materials 2019, 53(26-27), 002199831984805, DOI: 10.1177/0021998319848055.

[33] Ajenifuja E., Odetola P., Popoola A.P.I., Popoola O., Spark plasma sintering and structural analysis of nickel-titanium/coconut shell powder metal matrix composites, Int. J. Adv. Manuf. Technol. 2020, 108, 11-12, 3465-3473, DOI: 10.1007/s00170-020-05634-x.

[34] Ujah C.O., Popoola A.P.I., Popoola O.M., Aigbodion V.S., Influence of CNTs addition on the mechanical, microstructural, and corrosion properties of Al alloy using spark plasma sintering technique, The International Journal of Advanced Manufacturing Technology 106(12), 2020, 2961-2969.

[35] Cahoon J.R., The determination of yield strength from hardness measurements, Metallurgical Transactions 1971, 2, 1979-1983.

[36] Abe J.O., Popoola O.M., Popoola A.P.I., Ajenifuja E., Adebiyi D.I., Application of Taguchi design method for optimization of spark plasma sintering process parameters for Ti-6Al-4V/h-BN binary composite, Engineering Research Express 2019, 1(2).

[37] Callister W.D., Rethwisch D.G., Materials Science and Engineering: An Introduction, Willey, 2018.

[38] Kumar V., Kumar V., Singh R., Parametric study of aluminium-rare earth based composites with improved hydrophobicity using response surface method, Integr. Med. Res. 2020, 9, 3, 4919-4932, DOI: 10.1016/j.jmrt.2020.03.011.

[39] Rajabi M., Khodai M.M., Askari N., Microwave-assisted sintering of Al-$ZrO_2$ nano-composites, Journal of Materials Science: Materials in Electronics 25(10), 2014, June, 4577--4584, DOI: 10.1007/s10854-014-2206-6.

[40] Dhekwar B.T., Mohanty A., Pradhan J., Nayak S., Investigation of mechanical properties of aluminium silicon carbide hybride metal matrix composite (Mmcs), International Journal of Research in Engineering and Science 2017, 5, 4, 88-105.

[41] Reddy P.V., Ramanjaneyulu P., Reddy B.V., Rao P.S., Simultaneous optimization of drilling responses using GRA on Al-6063/TiC composite, SN Appl. Sci. 2020, 2, 3, 1-10, DOI: 10.1007/s42452-020-2214-5.

[42] Sumankant Y., Jawalkar C.S., Verma A.S., Suri N.M., Fabrication of aluminium metal matrix composites with

particulate reinforcement: A review, Mater. Today Proc. 2017, 4, 2, 2927-2936, DOI: 10.1016/j.matpr.2017.02.174.

[43] Saravanan C. et al., Investigation on the mechanical, tribological, morphological and machinability behavior of stir-casted Al/SiC/Mo reinforced MMCs, Mater. Today Proc. 2020, 21, 1-10, DOI: 10.1016/j.ceramint.2020.01.192.

[44] Hugar N. et al., Fabrication and characterization of high performance aluminium composites for automotive components, AIP Conf. Proc. 2022, 2421, 1-8, DOI: 10.1063/5.0076769.

[45] Yeshiye T., Gizaw M., A review on effects of reinforcements on properties and wear behaviour of aluminium metal matrix material, International Journal of Research in Engineering Technology 2021, 6, 2, March, 1-17.

[46] Mohammadpour M., Azari Khosroshahi R., Taherzadeh Mousavian R., Brabazon D., Effect of interfacial-active elements addition on the incorporation of micron-sized SiC particles in molten pure aluminum, Ceram. Int. 2014, 40, 6, 8323-8332, DOI: 10.1016/j.ceramint.2014.01.038.

[47] Kumar D., Angra S., Singh S., High-temperature dry sliding wear behavior of hybrid aluminum composite reinforced with ceria and graphene nanoparticles, Eng. Fail Anal. 2023, 151, May, 107426, DOI: 10.1016/j.engfailanal.2023.107426.

[48] Prakash B., Sivananthan S., Vijayan V., Investigation on mechanical properties of Al6061 alloy – Multiwall carbon nanotubes reinforced composites by powder metallurgy route, Mater. Today Proc. 2020, 37(15-16), 4-8, DOI: 10.1016/j.matpr.2020.04.907.

[49] Sharma V.K., Kumar V., Joshi R.S., Investigation of rare earth particulate on tribological and mechanical properties of Al-6061 alloy composites for aerospace application, Integr. Med. Res. 2019, 8, 4, 3504-3516, DOI: 10.1016/j.jmrt.2019.06.025.

[50] Baradeswaran A., Elaya Perumal A., Study on mechanical and wear properties of Al 7075/$Al_2O_3$/graphite hybrid composites, Compos. Part B Eng. 2014, 56, 464-471, DOI: 10.1016/j.compositesb.2013.08.013.

[51] Saravanan M., Pillai R.M., Ravi K.R., Pai B.C., Brahmakumar M., Development of ultrafine grain aluminium-graphite metal matrix composite by equal channel angular pressing, Compos. Sci. Technol. 2007, 67, 6, 1275-1279, DOI: 10.1016/j.compscitech.2006.10.003.

[52] Lata S., Pandey A., Sharma A., Meena K., An experimental study and analysis of the mechanical properties of titanium dioxide reinforced aluminum (AA 5051) composite, Mater. Today Proc. 2018, 5, 2, 6090-6097, DOI: 10.1016/j.matpr.2017.12.214.

[53] Amouri K., Kazemi S., Momeni A., Kazazi M., Microstructure and mechanical properties of Al-nano/micro SiC composites produced by stir casting technique, Mater. Sci. Eng. A 2016, 674, 569-578, DOI: 10.1016/ j.msea.2016.08.027.

[54] Abdizadeh H., Baghchesara M.A., Investigation into the mechanical properties and fracture behavior of A356 aluminum alloy-based $ZrO_2$-particle-reinforced metal--matrix composites, Mech. Compos. Mater. 2013, 49, 5, 571-576, DOI: 10.1007/s11029-013-9373-z.

[55] Moharana G.B., Senapati A.K., Tribological analysis of Al- Si alloy based MMCs at elevated temperature, Mater. Today Proc. 2021, 49, 1749-1755, DOI: 10.1016/j.matpr.2021.08.008.

[56] Ali M., Review of stir casting technique and technical challenges for ceramic reinforcement particulate and aluminium matrix composites, Epa – J. Silic Based Compos. Mater. 2020, 72, 6, 198-204, DOI: 10.14382/epitoanyag-jsbcm.2020.32.

[57] Munasir N., Triwikantoro T., Zainuri M., Bäßler R., Darminto D., Corrosion polarization behavior of Al-$SiO_2$ composites in 1M and related microstructural analysis, Int. J. Eng. 2019, 32, 7, 982-990, DOI: 10.5829/ije.2019.32.07a.11.

[58] Bhoi N.K., Singh H., Pratap S., Jain P.K., Aluminum yttrium oxide metal matrix composite synthesized by microwave hybrid sintering: processing, microstructure and mechanical response, J. Inorg. Organomet. Polym. Mater. 2022, DOI: 10.1007/s10904-021-02195-8.

[59] Sharma V.K., Kumar V., Joshi R.S., Experimental investigation on effect of RE oxides addition on tribological and mechanical properties of Al-6063 based hybrid composites Experimental investigation on effect of RE oxides addition on tribological and mechanical properties of Al-6063 based h, Mater. Res. Express 2019, 6, 8, 0865d7, DOI: 10.1088/2053-1591/ab2504.

[60] Kumar D., Singh S., Angra S., Dry sliding wear and microstructural behavior of stir-cast Al6061-based composite reinforced with cerium oxide and graphene nanoplatelets, Wear 2022, 516-517, September, 204615, DOI: 10.1016/j.wear.2022.204615.

[61] Bannigidad P., Aluminium oxide ($Al_2O_3$) nanopore image analysis using digital image processing techniques, 2017 Int. Conf. Comput. Commun. Control Autom., 1-4.

[62] Krishnamurthy K., Ashebre M., Venkatesh J., Suresha B., Dry sliding wear behavior of aluminum 6063 composites reinforced with $TiB_2$ particles, Journal of Minerals and Materials Characterization and Engineering 2017, 05(02), 74-89, DOI: 10.4236/jmmce.2017.52007.